
Unsupervised Learning with Stein’s Unbiased Risk Estimator

Christopher A. Metzler
Stanford University
cmetzler@stanford.edu

Ali Mousavi
Google AI
alimous@google.com

Reinhard Heckel
Rice University
rh43@rice.edu

Richard G. Baraniuk
Rice University
richb@rice.edu

Abstract

Learning from unlabeled and noisy data is one of the grand challenges of machine learning. As such, it has seen a flurry of research with new ideas proposed continuously. In this work, we revisit a classical idea: Stein’s Unbiased Risk Estimator (SURE). We show that, in the context of image recovery, SURE and its generalizations can be used to train convolutional neural networks (CNNs) for a range of image denoising and recovery problems *without any ground truth data*.

Specifically, our goal is to reconstruct an image \mathbf{x} from a *noisy* linear transformation (measurement) of the image. We consider two scenarios: one where no additional data is available and one where we have noisy measurements of other images that belong to the same distribution as \mathbf{x} , but have no access to the clean images. Such is the case, for instance, in the context of medical imaging, microscopy, and astronomy, where noise-less ground truth data is rarely available.

We show that in this situation, SURE can be used to estimate the mean-squared-error loss associated with an estimate of \mathbf{x} . Using this estimate of the loss, we train networks to perform denoising and compressed sensing recovery. In addition, we also use the SURE framework to partially explain and improve upon an intriguing result presented by Ulyanov et al. in [1]: that a network initialized with random weights and fit to a single noisy image can effectively denoise that image.

Public implementations of the networks and methods described in this paper can be found at https://github.com/ricedsp/D-AMP_Toolbox.

1 Introduction

In this work we consider reconstructing an unknown image $\mathbf{x} \in \mathbb{R}^n$ from measurements of the form $\mathbf{y} = \mathbf{H}\mathbf{x} + \mathbf{w}$, where $\mathbf{y} \in \mathbb{R}^m$ are the measurements, $\mathbf{H} \in \mathbb{R}^{m \times n}$ is the linear measurement operator, and $\mathbf{w} \in \mathbb{R}^m$ denotes noise. This problem arises in numerous applications, including denoising, inpainting, superresolution, deblurring, and compressive sensing. The goal of an image recovery algorithm is to use prior information about the image’s distribution and knowledge of the measurement operator \mathbf{H} to reconstruct \mathbf{x} .

The key determinant of an image recovery algorithm’s accuracy is the accuracy of its prior. Accordingly, over the past decades a large variety of increasingly complex image priors have been considered, ranging from simple sparse models [2], to non-local self-similarity priors [3], all the way to neural network based priors, in particular CNN based priors [4]. Among these methods, CNN priors often offer the best performance. It is widely believed that key to the success of CNN based

priors is the ability to process and learn from vast amounts of training data, although recent work suggests the structure of a CNN itself encodes strong prior information [1].

CNN image recovery methods are typically trained by taking a representative set of images $\mathbf{x}_1, \mathbf{x}_2, \dots, \mathbf{x}_L$, drawn from the same distribution as \mathbf{x} , and capturing a set of measurements $\mathbf{y}_1, \mathbf{y}_2, \dots, \mathbf{y}_L$, either physically or in simulation. The network then learns the mapping $f_\theta : \mathbf{y} \rightarrow \hat{\mathbf{x}}$ from observations back to images by minimizing a loss function; typically the mean-squared-error (MSE) between $f_\theta(\mathbf{y})$ and \mathbf{x} . This presents a challenge in applications where we do not have access to example images. Moreover, even if we have example images, we might have a large set of measurements as well, and would like to use that set to refine our reconstruction algorithm.

In the nomenclature of machine learning, the measurements \mathbf{y} would be considered features and the images \mathbf{x} the labels. Thus when $\mathbf{H} = \mathbf{I}$ the training problem simplifies to learning from noisy labels. When $\mathbf{H} \neq \mathbf{I}$ the training problem is to learn from noisy linear transformations of the labels.

Learning from noisy labels has been extensively studied in the context of classification; see for instance [5–9]. However, the problem of learning from noisy data has been studied far less in the context of image recovery. In this work we show that the SURE framework can be used to i) denoise an image with a neural network (NN) without any training data, ii) train NNs to denoise images from noisy training data, and iii) train a NN, using only noisy measurements, to solve the compressive sensing problem.

Two concurrent and independently developed works overlap with some of our contributions. Specifically, [10] demonstrates that SURE can be used to train CNN based denoisers without ground truth data and [11] demonstrates that SURE can be used to train CNNs for compressive sensing using only noisy compressive measurements.

2 SURE and its Generalizations

The goal of this work is to reconstruct an image \mathbf{x} from a noisy linear observations $\mathbf{y} = \mathbf{H}\mathbf{x} + \mathbf{w}$, and knowledge of the linear measurement operator \mathbf{H} . In addition to (\mathbf{y}, \mathbf{H}) , we assume that we are given training measurements $\mathbf{y}_1, \mathbf{y}_2, \dots, \mathbf{y}_L$ but not the images $\mathbf{x}_1, \mathbf{x}_2, \dots, \mathbf{x}_L$ that produced them (we also consider the case where no training measurements are given). Without access to $\mathbf{x}_1, \mathbf{x}_2, \dots, \mathbf{x}_L$ we cannot fit a model that minimizes the MSE, but we can minimize a loss based on Stein’s Unbiased Risk Estimator (SURE). In this section, we introduce SURE and its generalizations.

SURE. SURE is a model selection technique that was first proposed by its namesake in [12]. SURE provides an unbiased estimate of the MSE of an estimator of the mean of a Gaussian distributed random vector, with unknown mean. Let \mathbf{x} denote a vector we would like to estimate from noisy observations $\mathbf{y} = \mathbf{x} + \mathbf{w}$ where $\mathbf{w} \sim \mathcal{N}(0, \sigma_w^2 \mathbf{I})$. Also, assume $f_\theta(\cdot)$ is a weakly differentiable function parameterized by θ which receives noisy observations \mathbf{y} as input and provides an estimate of \mathbf{x} as output. Then, according to [12], we can write the expectation of the MSE with respect to the random variable \mathbf{w} as

$$\mathbb{E}_{\mathbf{w}} \left[\frac{1}{n} \|\mathbf{x} - f_\theta(\mathbf{y})\|^2 \right] = \mathbb{E}_{\mathbf{w}} \left[\frac{1}{n} \|\mathbf{y} - f_\theta(\mathbf{y})\|^2 \right] - \sigma_w^2 + \frac{2\sigma_w^2}{n} \text{div}_{\mathbf{y}}(f_\theta(\mathbf{y})), \quad (1)$$

where $\text{div}(\cdot)$ stands for divergence and is defined as

$$\text{div}_{\mathbf{y}}(f_\theta(\mathbf{y})) = \sum_{n=1}^N \frac{\partial f_{\theta n}(\mathbf{y})}{\partial y_n}. \quad (2)$$

Note that two terms within the SURE loss (1) depend on the parameter θ . The first term, $\frac{1}{n} \|\mathbf{y} - f_\theta(\mathbf{y})\|^2$ minimizes the difference between the estimate and the observations (bias). The second term, $\frac{2\sigma_w^2}{n} \text{div}_{\mathbf{y}}(f_\theta(\mathbf{y}))$ penalizes the denoiser for varying as the input is changed (variance). Thus SURE is a natural way to control the bias variance trade-off of a recovery algorithm.

The central challenge in using SURE in practice is computing the divergence. With advanced denoisers the divergence is hard or even impossible to express analytically.

Monte-Carlo SURE. MC-SURE is a Monte Carlo method to estimate the divergence, and thus the SURE loss, that was proposed in [13]. In particular, the authors show that for bounded functions f_θ we have

$$\operatorname{div}_{\mathbf{y}}(f_\theta(\mathbf{y})) = \lim_{\epsilon \rightarrow 0} \mathbb{E}_{\mathbf{b}} \left\{ \mathbf{b}^t \left(\frac{f_\theta(\mathbf{y} + \epsilon \mathbf{b}) - f_\theta(\mathbf{y})}{\epsilon} \right) \right\}, \quad (3)$$

where \mathbf{b} is an i.i.d. Gaussian distributed random vector with unit variance elements.

Following the law of large numbers, this expectation can be approximated with Monte Carlo sampling. Thanks to the high dimensionality of images, a single sample well approximates the expectation. The limit can be approximated well by using a small value for ϵ ; we use $\epsilon = \frac{\max(\mathbf{y})}{1000}$ throughout. This approximation leaves us with

$$\operatorname{div}_{\mathbf{y}}(f_\theta(\mathbf{y})) \approx \mathbf{b}^t \left(\frac{f_\theta(\mathbf{y} + \epsilon \mathbf{b}) - f_\theta(\mathbf{y})}{\epsilon} \right). \quad (4)$$

Combining the SURE loss (1) with the estimate of the divergence (4), enables minimization of the MSE of a denoising algorithm without ground truth data.

Generalized SURE. GSURE was proposed in [14] to estimate the MSE associated with estimates of \mathbf{x} from a linear measurement $\mathbf{y} = \mathbf{H}\mathbf{x} + \mathbf{w}$, where $\mathbf{H} \neq \mathbf{I}$, and \mathbf{w} has known covariance and follows any distribution from the exponential family. For the special case of i.i.d. Gaussian distributed noise the estimate simplifies to

$$\mathbb{E}_{\mathbf{w}} \left[\frac{1}{n} \|\mathbf{P}\mathbf{x} - \mathbf{P}f_\theta(\mathbf{y})\|^2 \right] = \mathbb{E}_{\mathbf{w}} \left[\frac{1}{n} \|\mathbf{P}\mathbf{x}\|^2 + \frac{1}{n} \|\mathbf{P}f_\theta(\mathbf{y})\|^2 + \frac{2\sigma_{\mathbf{w}}^2}{n} \operatorname{div}_{\mathbf{y}}(f_\theta(\mathbf{y})) - \frac{2}{n} f_\theta(\mathbf{y})^t \mathbf{H}^\dagger \mathbf{y} \right], \quad (5)$$

where \mathbf{P} denotes orthonormal projection onto the range space of \mathbf{H} and \mathbf{H}^\dagger is the pseudoinverse of \mathbf{H} . Note that while this expression involves the unknown \mathbf{x} , it can be minimized with respect to θ without knowledge of \mathbf{x} .

Propagating Gradients. Minimizing SURE requires propagating gradients with respect to the Monte Carlo estimate of the divergence (4). This is challenging to do by hand, but made easy by TensorFlow's and PyTorch's auto-differentiation capabilities, which are used throughout much of our experiments below.

3 Denoising Without Training Data

CNNs offer state-of-the-art performance for many image recovery problems including super-resolution [15], inpainting [16], and denoising [4]. Typically, these networks are trained on a large dataset of images. However, it was recently shown that if just fit to a single corrupted image \mathbf{y} , without any pre-training, CNNs can still perform effective image recovery. Specifically, the recent work *Deep Image Prior* [1] demonstrated that a randomly initialized CNN, trained so that its output matches the corrupted image \mathbf{y} well, performs exceptionally well at the aforementioned inverse problems. Similar to more traditional image recovery methods like BM3D [3], the deep image prior method only exploits structure within a given image and does not use any external training data.

3.1 Deep Image Prior

The deep image prior is a CNN, denoted by f_θ and parameterized by the weight and bias vector θ that maps an input tensor \mathbf{z} to an image $f_\theta(\mathbf{z})$. The paper [1] proposes to minimize

$$E(f_\theta(\mathbf{z}), \mathbf{y}),$$

over the parameters θ , starting from a random initialization, using a method such as gradient descent. Here, E is a loss function, chosen as the squared ℓ_2 -norm, i.e., $E(\mathbf{x}, \mathbf{x}') = \|\mathbf{x} - \mathbf{x}'\|_2^2$. In this paper, we consider a variant of the original Deep Image Prior work, where \mathbf{z} is set equal to \mathbf{y} .¹

¹As observed in [1], we found that perturbing the input slightly at every iteration helped with convergence. We will return to this observation in Section 7.

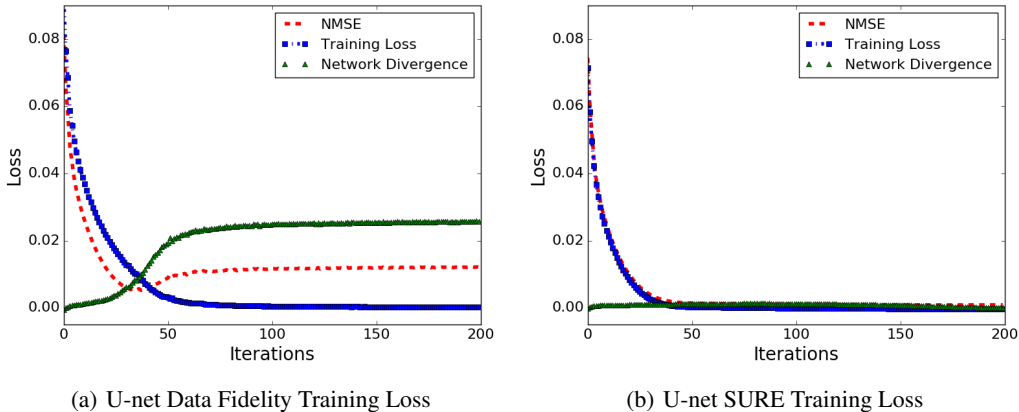


Figure 1: The training and test errors for networks trained with $\frac{1}{n}\|\mathbf{y} - f_{\theta}(\mathbf{y})\|^2$ Loss (a) and the SURE Loss (1) (b). Without the SURE divergence term, the network starts to overfit and the NMSE worsens even while the training loss improves. Minimizing the SURE loss minimizes the NMSE.

Following [1], our goal is to train the network, i.e., optimize the parameters θ , such that it fits the image but not the noise. If the network is trained using too few iterations, then the network does not represent the image well. If the network is trained until convergence, however, then the network’s parameters are overfit and describe the noise along with the actual image.

Thus, there is a sweet spot, where the network minimizes the error between the true image and the reconstructed image. This is illustrated in Figure 1(a). Figure 1(a) displays the training loss and NMSE associated with denoising a 512×512 Mandrill image which was contaminated with additive white Gaussian noise (AWGN) with standard deviation 25. It also displays the divergence of the network (3) (scaled by $2\sigma_w^2/n$). The figure shows that after a few iterations the network begins to overfit to the noisy image and normalized MSE (NMSE) starts to increase. Unfortunately, by itself the training loss gives little indication about when to stop training; it smoothly decays towards 0.

The network, f_{θ} , used to generate the results in this section was a very large U-net architecture [17] with 128 feature channels per layer. We set its input tensor \mathbf{z} to \mathbf{y} ; that is, the network was fed the noisy observation \mathbf{y} as an input. This network architecture was used in the “flash-no flash” experiments from [1], and offers performance incrementally better than the expansive CNN fed with a random \mathbf{z} the authors used for denoising experiments. We used this network architecture as it allows us to compute the divergence using the Monte-Carlo approximation (4). Qualitatively, our network behaves the same as network originally used for denoising in [1]; both require early stopping to achieve optimal performance.

3.2 SURE Deep Image Prior

Returning to Figure 1(a), we observe that the MSE is minimized at a point where the training loss is reasonably small, but at the same time the network divergence is not too large; thus the sum of the two terms is small. In fact, if one plots the SURE estimate of the loss (not shown here), it lies directly on top of the observed NMSE.

Inspired by this observation, we propose to train with the SURE loss instead of the fidelity or ℓ_2 loss. The results are shown in Figure 1(b). It can be seen that not only does the network avoid overfitting, the final NMSE is superior to that achieved by optimal stopping with the fidelity loss.

We tested the performance of this large U-net “trained” only on the image to be denoised against state-of-the-art trained and untrained algorithms DnCNN [4] and CBM3D [3]. Results are presented in Figure 2. When trained with the SURE loss the U-net trained only on the image to be denoised offers performance competitive with these two methods. However, the figure also demonstrates that

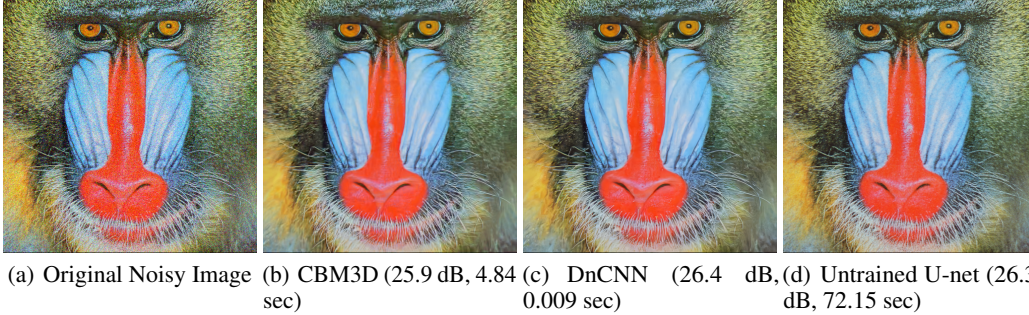


Figure 2: Reconstructions of 512×512 color Mandrill test image tested with AWGN with standard deviation 25. The untrained CNN offers performance similar to state-of-the-art methods but takes much longer.

the deep image prior method is very slow and that training across additional images, as exemplified by DnCNN, is beneficial.²

The networks described in this section were trained using the Adam optimizer [18] with a learning rate of 0.001. Throughout the paper we report recovery accuracies in terms of PSNR, defined as

$$\text{PSNR} = 10 \log_{10} \left(\frac{255^2}{\|\hat{x} - x\|^2} \right),$$

where all images lie in the range $[0, 255]$. All experiments were performed on a desktop with an Intel 6800K CPU and an Nvidia Pascal Titan X GPU.

4 Denoising with Noisy Training Data

In the previous section we showed that SURE can be used to fit a CNN denoiser without training data. This is useful in regimes where no training data whatsoever is available. However, as the previous section demonstrated, these untrained neural networks are computationally very expensive to apply.

In this section we focus on the scenario where we can capture additional *noisy* training data with which to train a neural network for denoising. We show that if provided a set of L *noisy* images $\mathbf{y}_1, \mathbf{y}_2, \dots, \mathbf{y}_L$, training the network with the SURE loss improves upon training with the MSE loss. Specifically, we optimize the network’s parameters by minimizing

$$\sum_{\ell=1}^L \frac{1}{n} \|\mathbf{y}_\ell - f_\theta(\mathbf{y}_\ell)\|^2 - \sigma_w^2 + \frac{2\sigma_w^2}{n} \text{div}_{\mathbf{y}_\ell} \{f_\theta(\mathbf{y}_\ell)\},$$

rather than

$$\sum_{\ell=1}^L \frac{1}{n} \|\mathbf{x}_\ell - f_\theta(\mathbf{y}_\ell)\|^2.$$

As before we will use the Monte-Carlo estimate of the divergence (3).

4.1 DnCNN and Experimental Setup

In this section, we consider the DnCNN image denoiser, trained on grayscale images pulled from Berkeley’s BSD-500 dataset [19], and trained using the MSE and SURE loss. Example images from this dataset are presented in Figure 3. The training images were cropped, rescaled, flipped, and rotated to form a set of 204 800 overlapping 40×40 patches. We tested the methods on 6 standard test images presented in Figure 4.

²In this section we used the DnCNN authors’ implementation of the algorithm. This implementation is faster than our own implementation, which is used elsewhere, but does not support auto-differentiation.

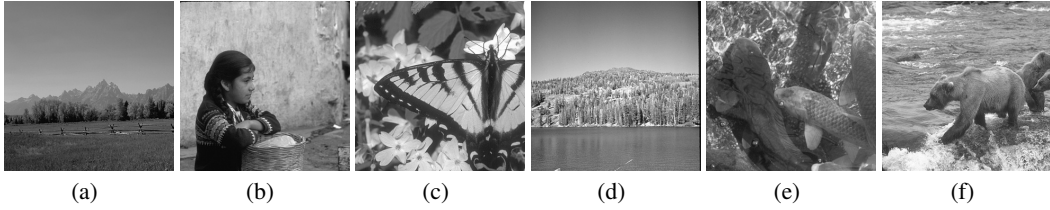


Figure 3: Six representative training images from the BSD dataset.

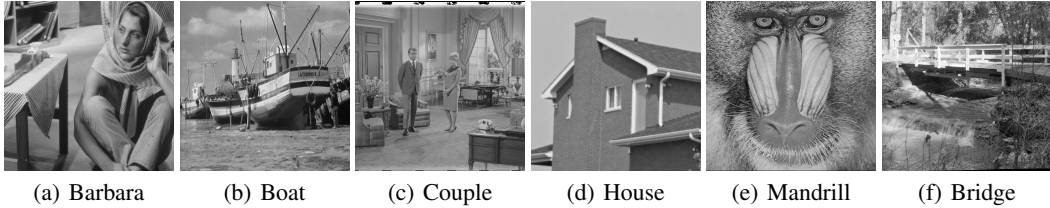


Figure 4: The six test images. They follow a similar distribution to the training images.

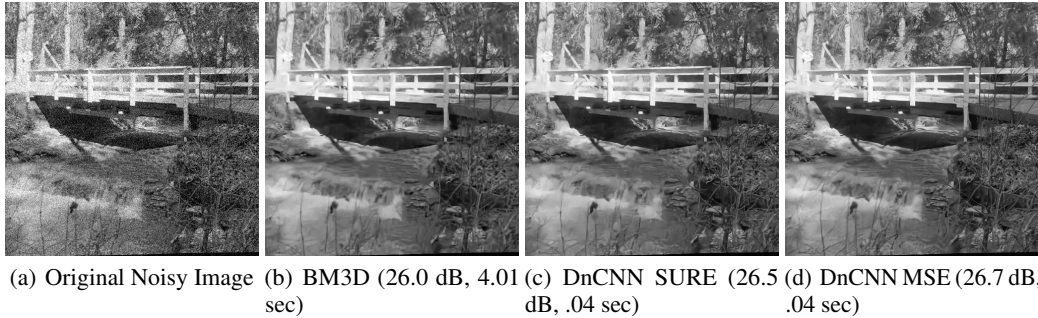


Figure 5: Reconstructions of 512×512 grayscale Bridge test image tested with AWGN with standard deviation 25. The CNN trained with noisy data offers performance similar to state-of-the-art methods.

The DnCNN image denoiser [4] consists of 16 sequential 3×3 convolutional layers with 64 features at each layer. Sandwiched between these layers are ReLU and batch-normalization operations. DnCNN has a single skip connection to its output and takes advantage of residual learning [20].

We trained all networks for 50 epochs using the Adam optimizer [18] with a training rate of 0.001 which was reduced to 0.0001 after 30 epochs. We used mini-batches of 128 patches.

Results. The results of training DnCNN using the MSE and SURE loss are presented in Figure 5 and Table 1. The results show that training DnCNN with SURE on noisy data results in reconstructions almost equivalent to training with the true MSE on clean images. Moreover, both DnCNN trained with SURE and with the true MSE outperform BM3D. As expected, because calculating the SURE loss requires two calls to the denoiser, it takes roughly twice as long to train as does training with the MSE.

5 Compressive Sensing Recovery with Noisy Training Measurements

In this section we study the problem of image recovery from undersampled linear measurements. The main novelty of this section is that we do not have training labels (i.e., ground truth images). Instead and unlike conventional learning approaches in compressive sensing (CS), we train the recovery algorithm using *only noisy undersampled linear measurements*.

	Training Time	Test Time	Barbara	Boat	Couple	House	Mandrill	Bridge
BM3D	N/A	0.82 sec	29.8	28.7	29.2	32.8	25.8	26.2
DnCNN SURE	8.1 hrs	0.01 sec	29.0	28.9	29.1	32.3	26.1	26.6
DnCNN MSE	4.3 hrs	0.01 sec	29.4	29.1	29.5	32.9	26.3	26.7

Table 1: Reconstruction results for 256×256 images with AWGN with standard deviation 25. Even though DnCNN SURE uses only noisy training data, it performs almost as well as the DnCNN MSE training on clean data. Results were averaged over 5 trials.

5.1 LDAMP

We used the Learned Denoising-based Approximate Message Passing (LDAMP) network proposed in [21] as our recovery method. LDAMP offers state-of-the-art CS recovery when dealing with measurement matrices with i.i.d. Gaussian distributed elements. LDAMP is an unrolled version of the DAMP [22] algorithm that decouples signal recovery into a series of denoising problems solved at every layer. In other words and as shown in (6), LDAMP receives a noisy version of \mathbf{x} (i.e., $\mathbf{x}^k + \mathbf{H}^* \mathbf{z}^k = \mathbf{x} + \sigma \boldsymbol{\nu}$) at every layer and tries to reconstruct \mathbf{x} by eliminating the effective noise vector $\sigma \boldsymbol{\nu}$.

The success of LDAMP stems from its Onsager correction term (i.e., the last term on the first line of (6)) that removes the bias from intermediate solutions. As a result, at each layer the effective noise term $\sigma \boldsymbol{\nu}$ follows a Gaussian distribution whose variance is accurately predicted by $(\sigma^k)^2$ [23].

Learned Denoising-based AMP (LDAMP) Neural Network
For $k = 1, \dots, K$

$$\begin{aligned} \mathbf{z}^k &= \mathbf{y} - \mathbf{H}\mathbf{x}^k + \frac{1}{m} \mathbf{z}^{k-1} \text{div} D_{\theta^{k-1}}^{k-1}(\mathbf{r}^{k-1}) \\ \sigma^k &= \frac{\|\mathbf{z}^k\|_2}{\sqrt{m}} \\ \mathbf{r}^k &= \mathbf{x}^k + \mathbf{H}^* \mathbf{z}^k \\ \mathbf{x}^{k+1} &= D_{\theta^k}^k(\mathbf{r}^k) \end{aligned} \quad (6)$$

In this work, we use a $K = 10$ layer LDAMP network, where each layer itself contains a 16 layer DnCNN denoiser $D_{\theta^k}^k(\cdot)$. Below we use $f_{\theta}(\cdot)$ to denote LDAMP.

5.2 Training LDAMP and Experimental Setup

We compare three methods of training LDAMP. All three methods utilize layer-by-layer training, which in the context of LDAMP is minimum MSE optimal [21].

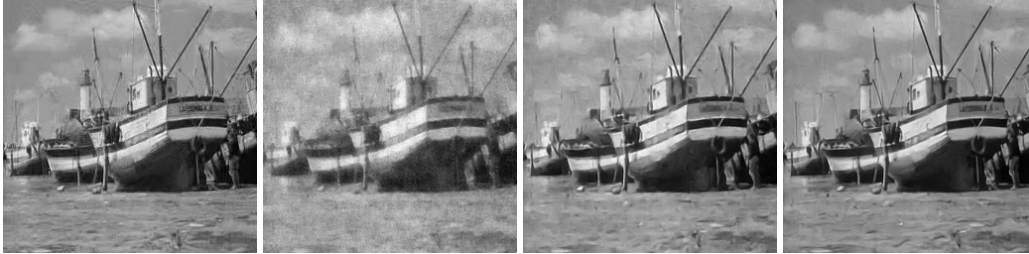
The first method, LDAMP MSE, simply minimizes the MSE with respect to the training data. The second method, LDAMP SURE, uses SURE to train LDAMP using only noisy measurements. This method takes advantage of the fact that at each layer LDAMP is solving denoising problems with known variance σ^{k^2} .

$$\theta_{\text{SURE}} = \arg \min_{\theta} \sum_{\ell=1}^L \frac{1}{n} \|\mathbf{r}_{\ell}^K - f_{\theta}(\mathbf{y}_{\ell})\|^2 - \sigma^{K^2} + \frac{2(\sigma^K)^2}{n} \text{div}_{\mathbf{y}_{\ell}}(f_{\theta}(\mathbf{y}_{\ell})).$$

The third and final method, LDAMP GSURE, uses generalized SURE to train LDAMP using only noisy measurements.

$$\theta_{\text{GSURE}} = \arg \min_{\theta} \sum_{\ell=1}^L \frac{1}{n} \|\mathbf{P} f_{\theta}(\mathbf{y}_{\ell})\|^2 + \frac{2\sigma_w^2}{n} \text{div}_{\mathbf{y}}(f_{\theta}(\mathbf{y}_{\ell})) - \frac{2}{n} f_{\theta}(\mathbf{y}_{\ell})^t \mathbf{H}^{\dagger} \mathbf{y}_{\ell}.$$

The SURE and GSURE methods both rely upon Monte-Carlo estimation of the divergence (3).



(a) BM3D-AMP (30.2 dB, 16.5 sec) (b) LDAMP GSURE (24.7 dB, 0.4 sec) (c) LDAMP SURE (29.5 dB, 0.4 sec) (d) LDAMP MSE (31.0 dB, 0.4 sec)

Figure 6: Reconstructions of 256×256 Boat test image sampled at a rate of $\frac{m}{n} = 0.2$ using modified fast JL transform matrices and i.i.d. Gaussian distributed measurement noise with standard deviation 1. LDAMP trained with SURE offers performance on par with BM3D-AMP.

	Training Time	Test Time	Barbara	Boat	Couple	House	Mandrill	Bridge
BM3D-AMP	N/A	16.5 sec	31.3	30.3	31.6	38.1	24.7	25.5
LDAMP SURE	34.7 hrs	0.4 sec	29.1	29.5	29.5	35.2	24.4	25.5
LDAMP GSURE	43.2 hrs	0.4 sec	25.2	24.5	24.7	28.2	23.0	22.9
LDAMP MSE	20.7 hrs	0.4 sec	30.2	31.0	31.6	36.4	24.9	25.9

Table 2: Reconstruction results for 256×256 images sampled at $\frac{m}{n} = 0.2$, using modified fast JL transform matrices with i.i.d. Gaussian noise with variance 1. Results were averaged over 5 trials.

We used $m \times n$ dense Gaussian measurement matrices for our low resolution training and modified “fast JL transform” matrices [24], which offer $O(n \log n)$ multiplications, for our high resolution testing.³ For both training and testing we sampled with $\frac{m}{n} = .2$ and $\sigma_w = 1$. See [21] for more details about the measurement process. Other experimental settings such as batch sizes, learning rates, etc. are the same as those in Section 4.1.

Results. The networks resulting from training LDAMP with the MSE, SURE, and GSURE losses are compared to BM3D-AMP [22] in Figure 6 and Table 2. The results demonstrate LDAMP networks trained with SURE and MSE both perform roughly on par with BM3D-AMP and run significantly faster. The results also demonstrate that LDAMP trained with GSURE offers significantly reduced performance. This can be understood by returning to the original GSURE cost (5). Minimizing GSURE minimizes the distance between $\mathbf{P}\mathbf{x}$ and $\mathbf{P}f_\theta(\mathbf{y})$ not between \mathbf{x} and $f_\theta(\mathbf{y})$, where \mathbf{P} denotes orthogonal projection onto the range space of \mathbf{H} . In the context of compressive sensing, the range space is small and so these two distances are not proportional to one another.

6 Related Work

Denoising and compressive sensing are each mature problems with vast literature. We list some of the most relevant works here.

Denoising with SURE SURE has a long history in the context of image denoising. For instance, it is the key ingredient in the well-known SureShrink wavelet denoising method [2], which uses SURE to set parameters in a wavelet-domain thresholding algorithm. SureShrink preceded a number of other wavelet-thresholding denoisers that have improved upon this basic idea [25, 26]. SURE and

³Our approximate “fast JL transform” matrices were of the form $\mathbf{H} = \mathbf{P}\mathbf{F}\mathbf{D}$ where \mathbf{P} is a sparse $m \times n$ matrix formed by randomly sampling the rows of an $n \times n$ identity matrix, \mathbf{F} is a Discrete Cosine Transform matrix, and \mathbf{D} is a diagonal matrices with i.i.d. entries that take values $-\sqrt{\frac{n}{m}}$ and $\sqrt{\frac{n}{m}}$ with probability .5.

related techniques have also been generalized and applied to Poisson [27], multiplicative [28], and other distributions [29] of noise.

Denoising with Noisy Training Data In [30], the authors used unbiased estimates of risk to train a neural network to denoise discrete-valued signals. In subsequent work, the authors used SURE to train a very simple neural network to denoise images [31]. [32] used noisy, blurry, and occluded images to train a GAN that could produce noise-free images. [33] demonstrated CNNs can be trained to restore images using *pairs* of corrupted training data, even without knowing the distribution of the noise.

Compressive Sensing The compressive sensing training/reconstruction method proposed in Section 5 is closely related to the projected GSURE method [34] and Parameterless Optimal AMP [35, 36], which use the (G)SURE loss to tune parallel coordinate descent and AMP [37] algorithms, respectively, to reconstruct signals with unknown sparsity in a known dictionary. The method is also closely related to Parametric SURE AMP [38] which uses SURE to adapt a parameterized denoiser at every iteration of the AMP algorithm.

The proposed method is somewhat related to blind CS [39] wherein signals that are sparse with respect to an unknown dictionary are reconstructed from compressive measurements. At a high level, the proposed method can be considered a practical form of universal CS [40–43] wherein a signal’s distribution is estimated from noisy linear measurements and then used to reconstruct the signal.

Other Applications We note in passing that unbiased risk estimators have seen use in a number of other applications including least squares estimation [44], kernel regression [45] and channel estimation [46].

7 Interpreting the Deep Image Prior

The original Deep Image Prior paper set out to minimize

$$\|\mathbf{y} - f_\theta(\mathbf{z})\|^2, \quad (7)$$

and attributed the success of the proposed method at least partly to the fact that the network fit the noise slower than than it fit the signal [1].

To minimize the cost function, the paper used an iterative first order method, specifically the ADAM optimizer. However, if tuned appropriately, one can use gradient descent and get essentially equivalent performance.

In either case, noise regularization dramatically improves the performance of the network. That is, [1] found it beneficial to add a noise vector γ , with $\gamma \sim N(0, \sigma_\gamma^2 \mathbf{I})$, at every iteration of the optimization. With this noise term, the optimization becomes equivalent to solving the stochastic optimization problem

$$\arg \min_{\theta} \mathbb{E}_\gamma \|\mathbf{y} - f_\theta(\mathbf{z} + \gamma)\|^2. \quad (8)$$

This has important implications. Using the techniques that [47] used to analyze denoising auto-encoders, we can take a Taylor expansion of f_θ around \mathbf{z} to express the loss function in (8) as

$$\begin{aligned} & \mathbb{E}_\gamma \left\| \mathbf{y} - f_\theta(\mathbf{z}) + \frac{\partial f_\theta(\mathbf{z})}{\partial \mathbf{z}} \gamma + o(\sigma_\gamma^2) \right\|^2 \\ &= \mathbb{E}_\gamma \left[\|\mathbf{y} - f_\theta(\mathbf{z})\|^2 - 2(\mathbf{z} - f_\theta(\mathbf{z}))^t \frac{\partial f_\theta(\mathbf{z})}{\partial \mathbf{z}} \gamma - 2(\mathbf{z} - f_\theta(\mathbf{z}))^t o(\sigma_\gamma^2) \right. \\ & \quad \left. + \gamma^t \frac{\partial f_\theta(\mathbf{z})}{\partial \mathbf{z}} \frac{\partial f_\theta(\mathbf{z})}{\partial \mathbf{z}} \gamma + 2\gamma^t \frac{\partial f_\theta(\mathbf{z})}{\partial \mathbf{z}} o(\sigma_\gamma^2) + o(\sigma_\gamma^4) \right] \\ &= \|\mathbf{y} - f_\theta(\mathbf{z})\|^2 - 2(\mathbf{z} - f_\theta(\mathbf{z}))^t \frac{\partial f_\theta(\mathbf{z})}{\partial \mathbf{z}} \mathbb{E}_\gamma[\gamma] + \text{Tr} \left(\mathbb{E}_\gamma[\gamma \gamma^t] \left[\frac{\partial f_\theta(\mathbf{z})}{\partial \mathbf{z}} \frac{\partial f_\theta(\mathbf{z})}{\partial \mathbf{z}} \right] \right) + o(\sigma_\gamma^2). \end{aligned}$$

Which, by substituting in $\mathbb{E}_\gamma[\gamma] = \mathbf{0}$ and $\mathbb{E}_\gamma[\gamma \gamma^t] = \sigma_\gamma^2 \mathbf{I}$, simplifies to

$$\|\mathbf{y} - f_\theta(\mathbf{z})\|^2 + \sigma_\gamma^2 \left\| \frac{\partial f_\theta(\mathbf{z})}{\partial \mathbf{z}} \right\|_F^2 + o(\sigma_\gamma^2) \text{ as } \sigma_\gamma \rightarrow 0. \quad (9)$$

As a consequence, the deep image prior can be interpreted as minimizing the loss function (9), as opposed to the loss function (7).

When $\mathbf{z} = \mathbf{y}$, as was the case in Section 3, this result can be understood geometrically. The Frobenius norm of the Jacobian penalizes the curvature of the loss function around \mathbf{y} : it encourages the vector field f_θ to be small around \mathbf{y} .

In contrast, training a network with the SURE loss, which does not require jittering the input, minimizes the cost

$$\|\mathbf{y} - f_\theta(\mathbf{y})\|^2 + 2\sigma_w^2 \sum_{n=1}^N \frac{\partial f_{\theta n}(\mathbf{y})}{\partial y_n}. \quad (10)$$

SURE penalizes the trace of the Jacobian. Geometrically, such a penalty encourages f_θ to be a sink at \mathbf{y} .

In either case, given enough parameters the network should be able to simultaneously set the data fidelity term $\|\mathbf{y} - f_\theta(\mathbf{y})\|^2$ to 0, that is fit the noisy signal \mathbf{y} exactly, while minimizing the regularization term. In fact, with the SURE loss, the network could ignore the data fidelity term entirely and focus on driving the divergence to negative infinity. Fortunately, in practice the learning dynamics are such that the solutions recovered by the network are stable for many hundreds of iterations.

8 Conclusions

We have made three distinct contributions. First we showed that SURE can be used to denoise an image using a CNN without any training data. Second, we demonstrated that SURE can be used to train a CNN denoiser using only noisy training data. Third, we showed that SURE can be used to train a neural network, using only noisy measurements, to solve the compressive sensing problem.

In the context of imaging, our work suggests a new hands-off approach to reconstruct images. Using SURE, one could toss a sensor into a novel imaging environment and have the sensor itself figure out and then apply the appropriate prior to reconstruct images.

In the context of machine learning, our work suggests that divergence may be an overlooked proxy for variance in an estimator. Thus, while SURE is applicable in only fairly specific circumstances, penalizing divergence could be applied more broadly as a tool to help attack overfitting.

References

- [1] D. Ulyanov, A. Vedaldi, and V. S. Lempitsky, “Deep image prior,” *CoRR*, vol. abs/1711.10925, 2017.
- [2] D. L. Donoho and I. M. Johnstone, “Adapting to unknown smoothness via wavelet shrinkage,” *Journal of the american statistical association*, vol. 90, no. 432, pp. 1200–1224, 1995.
- [3] K. Dabov, A. Foi, V. Katkovnik, and K. Egiazarian, “Image denoising by sparse 3-d transform-domain collaborative filtering,” *IEEE Transactions on image processing*, vol. 16, no. 8, pp. 2080–2095, 2007.
- [4] K. Zhang, W. Zuo, Y. Chen, D. Meng, and L. Zhang, “Beyond a gaussian denoiser: Residual learning of deep cnn for image denoising,” *IEEE Transactions on Image Processing*, vol. 26, no. 7, pp. 3142–3155, 2017.
- [5] N. Natarajan, I. S. Dhillon, P. K. Ravikumar, and A. Tewari, “Learning with noisy labels,” in *Proc. Adv. in Neural Processing Systems (NIPS)*, 2013, pp. 1196–1204.
- [6] T. Xiao, T. Xia, Y. Yang, C. Huang, and X. Wang, “Learning from massive noisy labeled data for image classification,” in *Proc. IEEE Int. Conf. Comp. Vision, and Pattern Recognition*, 2015, pp. 2691–2699.
- [7] T. Liu and D. Tao, “Classification with noisy labels by importance reweighting,” *IEEE Trans. Pattern Anal. Machine Intell.*, vol. 38, no. 3, pp. 447–461, 2016.
- [8] S. Sukhbaatar, J. Bruna, M. Paluri, L. Bourdev, and R. Fergus, “Training convolutional networks with noisy labels,” *arXiv preprint arXiv:1406.2080*, 2014.
- [9] S. Sukhbaatar and R. Fergus, “Learning from noisy labels with deep neural networks,” *arXiv preprint arXiv:1406.2080*, vol. 2, no. 3, p. 4, 2014.

- [10] S. Soltanayev and S. Y. Chun, “Training deep learning based denoisers without ground truth data,” in *Advances in Neural Information Processing Systems*, 2018, pp. 3257–3267.
- [11] M. Zhussip and S. Y. Chun, “Simultaneous compressive image recovery and deep denoiser learning from undersampled measurements,” *arXiv preprint arXiv:1806.00961*, 2018.
- [12] C. M. Stein, “Estimation of the mean of a multivariate normal distribution,” *The annals of Statistics*, pp. 1135–1151, 1981.
- [13] S. Ramani, T. Blu, and M. Unser, “Monte-carlo sure: A black-box optimization of regularization parameters for general denoising algorithms,” *IEEE Transactions on Image Processing*, vol. 17, no. 9, pp. 1540–1554, 2008.
- [14] Y. C. Eldar, “Generalized sure for exponential families: Applications to regularization,” *IEEE Transactions on Signal Processing*, vol. 57, no. 2, pp. 471–481, 2009.
- [15] C. Dong, C. Loy, K. He, and X. Tang, “Learning a deep convolutional network for image super-resolution,” in *European Conference on Computer Vision*. Springer, 2014, pp. 184–199.
- [16] C. Yang, X. Lu, Z. Lin, E. Shechtman, O. Wang, and H. Li, “High-resolution image inpainting using multi-scale neural patch synthesis,” in *The IEEE Conference on Computer Vision and Pattern Recognition (CVPR)*, vol. 1, no. 2, 2017, p. 3.
- [17] O. Ronneberger, P. Fischer, and T. Brox, “U-net: Convolutional networks for biomedical image segmentation,” in *International Conference on Medical image computing and computer-assisted intervention*. Springer, 2015, pp. 234–241.
- [18] D. Kingma and J. Ba, “Adam: A method for stochastic optimization,” *arXiv preprint arXiv:1412.6980*, 2014.
- [19] D. Martin, C. Fowlkes, D. Tal, and J. Malik, “A database of human segmented natural images and its application to evaluating segmentation algorithms and measuring ecological statistics,” *Proc. Int. Conf. Computer Vision*, vol. 2, pp. 416–423, July 2001.
- [20] K. He, X. Zhang, S. Ren, and J. Sun, “Deep residual learning for image recognition,” *Proc. IEEE Int. Conf. Comp. Vision, and Pattern Recognition*, pp. 770–778, 2016.
- [21] C. Metzler, A. Mousavi, and R. Baraniuk, “Learned d-amp: Principled neural network based compressive image recovery,” in *Advances in Neural Information Processing Systems*, 2017, pp. 1770–1781.
- [22] C. A. Metzler, A. Maleki, and R. G. Baraniuk, “From denoising to compressed sensing,” *IEEE Transactions on Information Theory*, vol. 62, no. 9, pp. 5117–5144, 2016.
- [23] A. Maleki, “Approximate message passing algorithm for compressed sensing,” *Stanford University PhD Thesis*, Nov. 2010.
- [24] N. Ailon and B. Chazelle, “Approximate nearest neighbors and the fast johnson-lindenstrauss transform,” in *Proceedings of the thirty-eighth annual ACM symposium on Theory of computing*. ACM, 2006, pp. 557–563.
- [25] T. Blu and F. Luisier, “The sure-let approach to image denoising,” *IEEE Transactions on Image Processing*, vol. 16, no. 11, pp. 2778–2786, 2007.
- [26] M. Raphan and E. P. Simoncelli, “Optimal denoising in redundant representations,” *IEEE Transactions on image processing*, vol. 17, no. 8, pp. 1342–1352, 2008.
- [27] F. Luisier, T. Blu, and M. Unser, “Image denoising in mixed poisson–gaussian noise,” *IEEE Transactions on image processing*, vol. 20, no. 3, pp. 696–708, 2011.
- [28] B. K. Panissetti, T. Blu, and C. S. Seelamantula, “An unbiased risk estimator for multiplicative noise—application to 1-d signal denoising,” in *2014 19th International Conference on Digital Signal Processing*. IEEE, 2014, pp. 497–502.
- [29] S. V. Gubbi and C. S. Seelamantula, “Risk estimation without using stein’s lemma—application to image denoising,” *arXiv preprint arXiv:1412.2210*, 2014.
- [30] T. Moon, S. Min, B. Lee, and S. Yoon, “Neural universal discrete denoiser,” in *Advances in Neural Information Processing Systems*, 2016, pp. 4772–4780.

- [31] S. Cha and T. Moon, “Neural adaptive image denoiser,” in *2018 IEEE International Conference on Acoustics, Speech and Signal Processing (ICASSP)*. IEEE, 2018, pp. 2981–2985.
- [32] A. Bora, E. Price, and A. G. Dimakis, “Ambientgan: Generative models from lossy measurements,” in *International Conference on Learning Representations (ICLR)*, 2018.
- [33] J. Lehtinen, J. Munkberg, J. Hasselgren, S. Laine, T. Karras, M. Aittala, and T. Aila, “Noise2Noise: Learning image restoration without clean data,” in *Proceedings of the 35th International Conference on Machine Learning*, ser. Proceedings of Machine Learning Research, J. Dy and A. Krause, Eds., vol. 80. Stockholmsmässan, Stockholm Sweden: PMLR, 10–15 Jul 2018, pp. 2971–2980.
- [34] R. Giryes, M. Elad, and Y. C. Eldar, “The projected gsure for automatic parameter tuning in iterative shrinkage methods,” *Applied and Computational Harmonic Analysis*, vol. 30, no. 3, pp. 407–422, 2011.
- [35] A. Mousavi, A. Maleki, and R. G. Baraniuk, “Parameterless optimal approximate message passing,” *arXiv preprint arXiv:1311.0035*, 2013.
- [36] M. Bayati, M. A. Erdogdu, and A. Montanari, “Estimating lasso risk and noise level,” in *Advances in Neural Information Processing Systems*, 2013, pp. 944–952.
- [37] D. L. Donoho, A. Maleki, and A. Montanari, “Message-passing algorithms for compressed sensing,” *Proceedings of the National Academy of Sciences*, vol. 106, no. 45, pp. 18 914–18 919, 2009.
- [38] C. Guo and M. E. Davies, “Near optimal compressed sensing without priors: Parametric sure approximate message passing,” *IEEE Trans. Signal Processing*, vol. 63, no. 8, pp. 2130–2141, 2015.
- [39] S. Gleichman and Y. C. Eldar, “Blind compressed sensing,” *IEEE Transactions on Information Theory*, vol. 57, no. 10, pp. 6958–6975, 2011.
- [40] S. Jalali, A. Maleki, and R. G. Baraniuk, “Minimum complexity pursuit for universal compressed sensing,” *IEEE Transactions on Information Theory*, vol. 60, no. 4, pp. 2253–2268, 2014.
- [41] D. Baron and M. F. Duarte, “Universal map estimation in compressed sensing,” in *Communication, Control, and Computing (Allerton), 2011 49th Annual Allerton Conference on*. IEEE, 2011, pp. 768–775.
- [42] J. Zhu, D. Baron, and M. F. Duarte, “Recovery from linear measurements with complexity-matching universal signal estimation,” *IEEE Trans. Signal Processing*, vol. 63, no. 6, pp. 1512–1527, 2015.
- [43] S. Jalali and H. V. Poor, “Universal compressed sensing for almost lossless recovery,” *IEEE Transactions on Information Theory*, vol. 63, no. 5, pp. 2933–2953, 2017.
- [44] M. Raphan and E. P. Simoncelli, “Least squares estimation without priors or supervision,” *Neural computation*, vol. 23, no. 2, pp. 374–420, 2011.
- [45] S. R. Krishnan, C. S. Seelamantula, and P. Chakravarti, “Spatially adaptive kernel regression using risk estimation,” *IEEE Signal Processing Letters*, vol. 21, no. 4, pp. 445–448, 2014.
- [46] K. Upadhyay, C. S. Seelamantula, and K. Hari, “A risk minimization framework for channel estimation in ofdm systems,” *Signal Processing*, vol. 128, pp. 78–87, 2016.
- [47] G. Alain and Y. Bengio, “What regularized auto-encoders learn from the data-generating distribution,” *The Journal of Machine Learning Research*, vol. 15, no. 1, pp. 3563–3593, 2014.